The Performance of LiF:Mg-Ti for Proton Dosimetry within the Framework of the MoVe IT Project

Vittoria D'Avino [1,2,*], Francesco Tommasino [3,4], Stefano Lorentini [5], Giuseppe La Verde [1,2] and Mariagabriella Pugliese [1,2]

1   Department of Physics "Ettore Pancini", University of Naples Federico II, 80126 Naples, Italy; laverde@na.infn.it (G.L.V.); pugliese@na.infn.it (M.P.)
2   National Institute for Nuclear Physics, INFN Section of Naples, 80126 Naples, Italy
3   Department of Physics, University of Trento, 38123 Trento, Italy; francesco.tommasino@unitn.it
4   Trento Institute for Fundamental Physics and Applications (TIFPA), National Institute for Nuclear Physics, INFN, 38123 Trento, Italy
5   Protontherapy Department, Azienda Provinciale per i Servizi Sanitari (APSS), 38122 Trento, Italy; stefano.lorentini@apss.tn.it
*   Correspondence: vittoria.davino@na.infn.it; Tel.: +39-081-676-221

Abstract: Proton therapy represents a technologically advanced method for delivery of radiation treatments to tumors. The determination of the biological effectiveness is one of the objectives of the MoVe IT (Modeling and Verification for Ion Beam Treatment Planning) project of the National Institute for Nuclear Physics (INFN) CSN5. The aim of the present work, which is part of the project, was to evaluate the performance of the thermoluminescent dosimeters (TLDs-100) for dose verification in the proton beam line. Four irradiation experiments were performed in the experimental room at the Trento Proton Therapy Center, where a 150 MeV monoenergetic proton beam is available. A total of 80 TLDs were used. The TLDs were arranged in one or two rows and accommodated in a specially designed water-equivalent phantom. In the experimental setup, the beam enters orthogonally to the dosimeters and is distributed along the proton beam profile, while the irradiation delivers doses of 0.8 Gy or 1.5 Gy in the Bragg peak. For each irradiation stage, the depth–dose curve was determined by the TLD readings. The results showed the good performance of the TLDs-100, proving their reliability for dose recordings in future radiobiological experiments planned within the MoVe IT context.

Keywords: TLD-100; proton beam radiation; dose verification; proton dosimetry

1. Introduction

Proton beam therapy (PBT) represents the election therapy for the treatment of many solid tumors [1,2]. Charged particles (protons or ions) show physical properties that give a more localized energy deposition with reference to conventional MV X-ray therapy. PBT treatment plans manage to maximize the tumor control probability while minimizing the damage to surrounding healthy tissues. The theoretical advantage over photon radiation lies within the depth–dose profile, referred to as the Bragg curve, culminating with a sharp decrease beyond the so-called Bragg peak, especially for protons. Consequently, the deposited dose increases steeply within a short distance nearing the end of the protons' range, resulting in high conformity to the tumor. In order to account for the difference in biological response between high linear energy transfer (LET) radiation and low LET radiation, the relative biological effectiveness (RBE) parameter was introduced. RBE is defined as the ratio of the absorbed dose of a usually low LET reference radiation (such as X-rays or Co-60 gamma rays) to the absorbed dose of an ionizing particle that produces the same biological effect. The RBE is a modifying factor that converts the physical dose into a biological equivalent dose. For protons, the International Commission on Radiation

Units [3] recommended that one assume the value of the RBE as being equal to 1.1, meaning that protons are 10% more effective than photons regarding the defined biological response; however, the use of a constant RBE of 1.1 by the proton therapy community is currently under debate [4]. Beyond the biological endpoint, RBE depends on many factors [5,6], such as the deposited physical dose, radiation quality (LET, type, energy), radiosensitivity of the irradiated tissue and cell type, dose rate, and oxygen concentration. Interestingly, the RBE of protons increases close to the field edges and beyond the distal Bragg peak, as LET increases moderately through the spread-out Bragg peak (SOBP) [5,7–11]. The spatial variation in RBE along the proton beam may have important clinical impacts regarding potential increases in treatment complications, because the distal edge of the SOBP could be situated within the surrounding normal tissue [12]; that is, an increase in RBE at the end of the proton range should be accounted for in treatment planning [13] in order to gain the optimum therapeutic advantage.

The knowledge of proton radiobiology is based on important information extracted from in vitro experiments using cell cultures [14–19]. New studies regarding the relative radiobiological effectiveness of proton irradiation should be carried out from in vivo, through which the generated hypotheses could be formed for the far more complex biology of patients; however, due to the associated costs and time required, few studies assessing the radiation effects of protons on in vivo models are available in the literature [20–22]. The scarcity of such in vivo experiments means the RBE issue remains unsolved.

Advances in particle therapy have meant that models are required for biologically optimized treatment planning systems (TPS) in ion beam therapy, as well as dedicated devices for plan verification that can account for a wide range of complex physical and biological effects. The present work lies within the framework of the MoVe IT project, aiming to exploit both modeling and verification methods for ion beam TPS, with a main focus on RBE, the biological impacts of nuclear fragmentation, and intra-tumor heterogeneity. This project involves interdisciplinary research, in which physical and radiobiological expertise are managed in 4 scientific work packages (WP). The results of this paper are gained from experimental activities included within WP3, which is targeted toward biological dosimetry. The goal of WP3 is the development of new devices for measurements of biological effects; that is, for RBE measurements and for radiobiological characterization of the proton beamline used for the exemplary selection of tissue types. A monoenergetic proton beam available in the experimental room at INFN-TIFPA (Trento Institute for Fundamental Physics and Applications) in the Proton Therapy Center was used to simultaneously irradiate the thermoluminescent dosimeters, which were provided and analyzed by the Naples Unit, while tumor cell lines were inserted in the bio-phantom designed by the BioTech (UniTN) partner. The accuracy and precision of the doses measured using TLD in the high-energy proton beams, in particular in the distal fall-off region of the Bragg peak, have been reported in several studies in the literature [23–30]. The results indicate that for all commonly used materials, the sensitivity (TL response or absorbed dose) decreases with increasing LET; however, it has been demonstrated that the sensitivity of the high temperature peak for TLD-100 in the proton beam is stable, allowing the accurate determination of doses to within ±4.0% [30]. This study reports the results of several exploratory tests of physical dosimetry along the proton beam profile to verify the performance of TLDs for radiobiological dosimetry. Depth–dose curves are reconstructed for several configurations and different planned dose values at the Bragg peak. The results of this investigation will help us to assess whether TLDs can be used as reliable in vivo dosimeters in proton beam therapy.

2. Materials and Methods

2.1. Proton Beam Trento Facility

The Trento Proton Therapy Center (PTC) is equipped with two medical treatment rooms and an experimental area that contains a research beam line dedicated to scientific applications, including medical physics, detector testing, and radiobiology. Consistent

with an institutional agreement with Trentino Healthcare Agency (Azienda Provinciale per i Servizi Sanitari, Italy), research activities are managed and supervised by INFN-TIFPA, who organize the Program Advisory Committee responsible for picking the access requests. After the beam production and acceleration by the cyclotron, an energy selection system reduces the cyclotron extraction energy to the desired value, and the beam can be directed either to the treatment gantries or to the experimental room. A fixed pencil beam line, in the energy range between 70 and 228 MeV, is available in the "physics" line of the research room. Energies below 70 MeV can be obtained using dedicated in-air degraders acting as pre-absorbers just ahead of the target. The passive scattering system implemented in the facility is based on the dual ring, which at the target position provided an irradiation field of 6 cm diameter with a dose uniformity >90%. An in-depth description of the experimental rooms at Trento PTC facility used for beam production and transport is available in [23,24].

2.2. Dosimeters, Annealing, and Readout Procedures

The TLDs are widely used in conventional radiation therapy [31–33], while their use in the field of clinical proton beam dosimetry is not currently a routine practice. Despite care being recommended when using TLDs within the distal-off region of the pristine Bragg peak, due to their energy and LET dependence, they are the choice for dosimetry of small fields in which negligible perturbation of the irradiation beam is required.

The TLD-100 chips (Harshaw Chemical Company, Cleveland, OH, USA) utilized in our investigation are the foremost common and cheapest thermoluminescent materials, containing a natural lithium composition (LiF:Mg, Ti). They have size of $3.2 \times 3.2 \times 0.89$ mm^3, spatial resolution of 2 mm, and density of 2.64 g/cm^3. This type of TLD has an effective atomic number equal to 8.2 [34], comparable to water (Zeff = 7.42 [35]), as well as a high sensitivity and linearity range that extends from 10 μGy up to 10 Gy, where the sub-linearity starts. These characteristics represent the main advantages for dosimetry applications, especially in clinical measurements [31,36,37].

Annealing of the TLD material before the irradiation was performed according to the standard procedure: 1 h heating in an oven at 400 °C; 2 h heating at 100 °C; cool-down to ambient temperature. Dosimeters were analyzed with a hot gas manual TLD reader, Harshaw model 3500, installed at the Department of Physics of the University of Naples Federico II. A dedicated software (Thermo Scientific *WinREMS*, Waltham, MA, USA) was used to set the acquisition setup parameters and to monitor the TLD readings. The time–temperature profile for each chip started when the gas was at 100 °C, at which point the gas temperature increased by 5 °C/s to a maximum of 300 °C, where it was held constant for 40 s, after which the gas was cooled to 100 °C before the subsequent chip was read. The photomultiplier charge was integrated over the temperature ramp-up and plateau regions of the heating profile. During the measurement process, a continuous nitrogen flow was used to reduce chemiluminescence and spurious signals not associated with the irradiation [38]. A total of 80 dosimeters from two batches of TLDs were used during MoVe IT activity (2017–2021).

2.3. TLD Characterization and Irradiation

The TLDs used were characterized and calibrated with photon, electron, and proton beams in the dose and energy range of interest for clinical applications. The calibration curves for all beams are reported in previously published studies [32,33,39]. According to the entrance energy into the bio-phantom used for the MoVe IT experiments, the corresponding calibration factor was applied to convert the responses of the TLDs to dose values. In order to obtain high spatial resolution dose information, the dosimeters were accommodated in a water-equivalent bio-phantom (Figure 1) designed to contain both TLDs and tumor cells in a gelatine developed for this purpose. The experimental setup ensured that the beam entered orthogonally to the bio-phantom. A schematic view and description of the irradiation configuration implemented in Trento for radiobiological experiments can be found in [24].
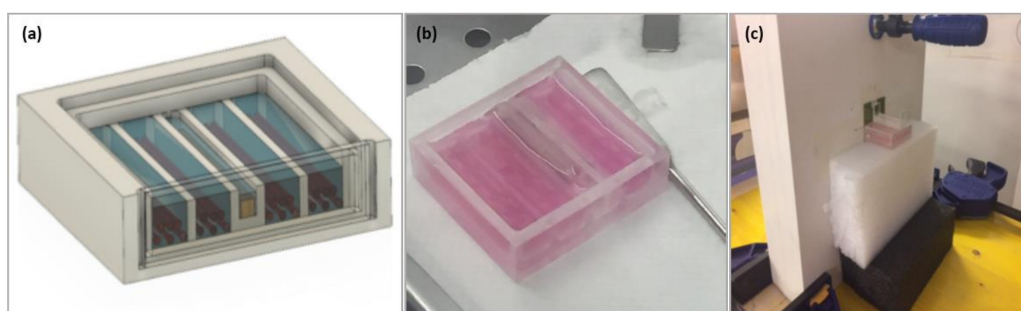
Figure 1. (**a**) Design of the bio-phantom implemented by the BioTech (UniTN) partner, containing both thermoluminescent dosimeters (TLDs-100) and cells. (**b**) Bio-phantom with an array of TLDs and cells included in the gelatine. (**c**) Bio-phantom ready for irradiation with the beam entering orthogonally.

The dosimeters were arranged in single or double rows (named row 1 and row 2). Eight dosimeters were not irradiated and were used to correct the TLD measures for the background signal.

The experiments reported in this study were performed between 2018 and 2020 and are described below. In the first irradiation stage (July 2018), only one bio-phantom was irradiated by a proton beam with an initial energy of 150 MeV (about 80 MeV on the phantom entrance) at a Bragg peak dose of 1.5 Gy. In the second irradiation stage (October 2018), two TLD rows were used, each positioned in a bio-phantom and irradiated one-by-one. The experimental setup of the first bio-phantom irradiation was the same as that adopted in the July experiment, while in the second bio-phantom the energy of the entrance proton beam was deliberately increased to observe the shift of the Bragg peak position in the TLD row. In the third and fourth irradiation stages (March and October 2020), one single TLD row was irradiated at the dose level with Bragg peaks of 1.5 Gy and 0.8 Gy, respectively.

2.4. Data Analysis

For each point dose profile measurement, the TLD response was converted into a dose value by applying the calibration and the corresponding error was calculated by taking into account the uncertainties of the calibration factor and thermoluminescent response provided by the TLD reader (5% of the reading). The depth position of each TLD was calculated by considering both the water-equivalent bio-phantom thickness (4 mm) before the beam entered into the TLD row and the water-equivalent thickness of the TLD material. The TLD dose response was finally plotted as a function of the water depth.

3. Results and Discussion

The depth–dose profiles resulting from the irradiation of the TLD rows are shown in Figure 2. Figure 2b (second experiment) shows an energy shift that resulted in a peak shift between the two TLD rows of about 7 mm, as we expected.

The first and the second experiments provided an entrance dose into the bio-phantom of 0.7 Gy, corresponding to a peak dose of 1.5 Gy for both rows. In the third experiment (Figure 2c), the entrance dose measure was 0.9 Gy, while for the fourth experiment (Figure 2d) it was 0.5 Gy (corresponding to peak doses of 1.5 Gy and 0.8 Gy, respectively). The depth–dose profile in Figure 2c shows a peak shifted at a lower depth than the other ones. A variation in the setup using a larger thickness for the water-equivalent slab phantom (RW3 slab phantom) affected the peak position, which was correctly detected by the dosimeters.

The depth–dose profiles obtained with TLDs-100 using the same geometrical configuration and beam parameters (first and second irradiation-row 1) are compared in Figure 3.
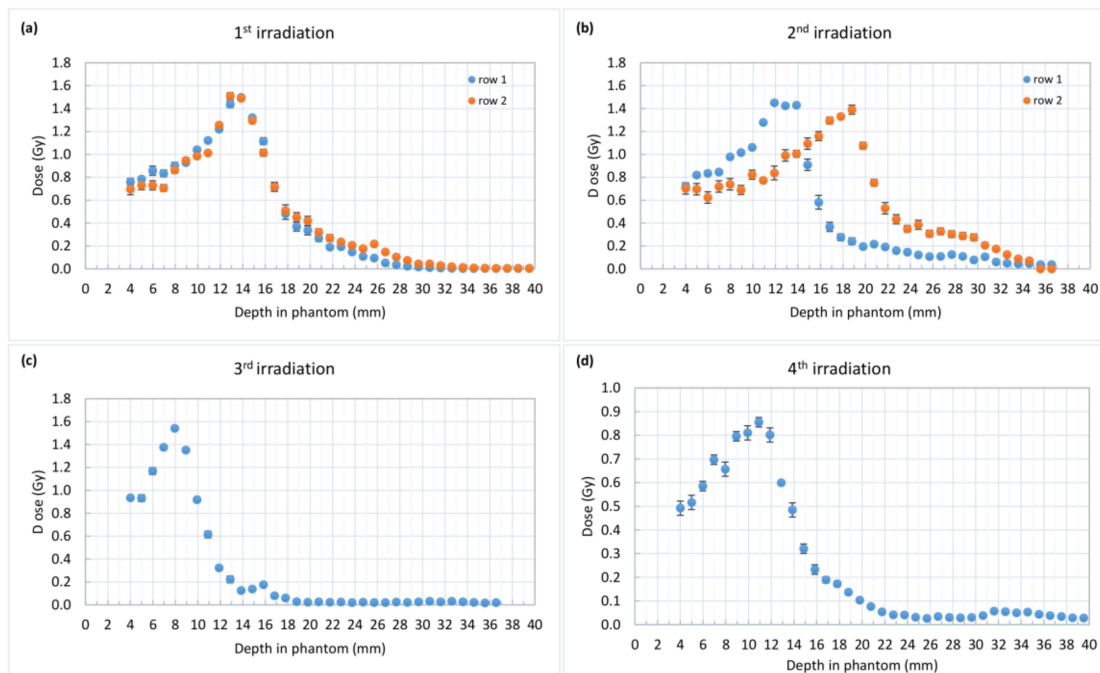
Figure 2. Depth–dose profiles of the proton beam in a bio-phantom provided by the thermoluminescent dosimeters (TLDs-100): (**a**) first irradiation stage: two TLDs' rows irradiated simultaneously; (**b**) second irradiation stage: two TLDs' rows irradiated one at time, the second one with a planned energy shift; (**c,d**) third and fourth irradiation stages: one TLD's row irradiated at different Bragg peak dose.
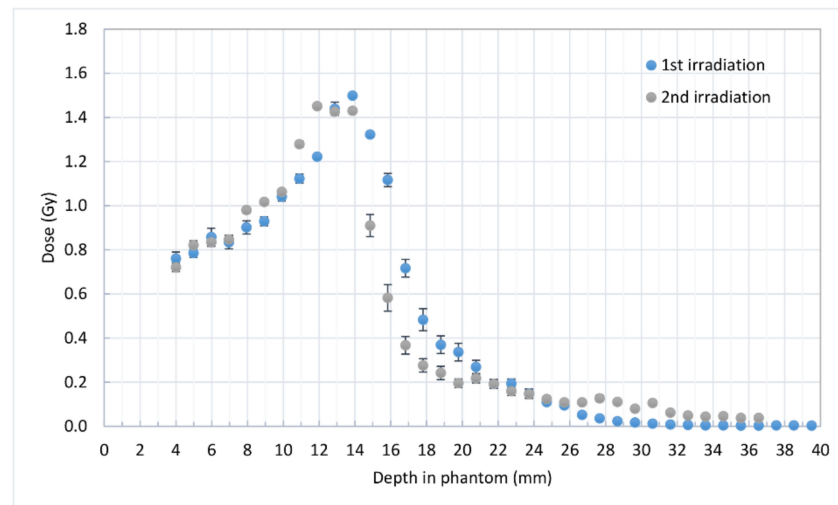
Figure 3. Comparison between proton beam depth–dose profiles reconstructed with the thermoluminescent dosimeters (TLDs-100) from row 1 in the 1st and 2nd irradiation stages.

High dose differences occurred in the distal fall-off region of the Bragg peak, while lower deviations were observed elsewhere.

A combination of several factors relating both to dosimeter characteristics and the proton beam dose profile can result in the deviation observed between the two measurements. First, the relative dose efficiency of TLDs depends on the activator (Mg, Ti) concentrations, batch-to-batch variations, and on the annealing process; thus, it should be determined for the TLD batch used in each specific dose measurement. In addition, the TLD efficiency for measuring the absorbed dose drops off as the linear energy transfer of the charged particles increases [40–43]. In the study by Zullo et al. [30], the dose measurements using TLD-100 in a proton beam in the distal fall-off region were accurate to within ±5.0%. The

data measured are in good agreement with the data from the literature, but it is important to point out that a comparison of the efficiency values gathered from different groups has to be performed very carefully owing to the different readout and evaluation procedures used by the research groups.

On the other hand, the reproducibility of the experiment is more critical in the steeply descending region downstream of the Bragg peak, while the flatness region is such that the TLD positioning accuracy has less impact on the absorbed dose variation. The knowledge of the Bragg peak position plays a key role in the correct delivery of proton therapy, since the setup uncertainties influence the proton range and dose distribution [44,45]. For this reason, the only strategy that can be used to catch treatments errors, assist in treatment adaptation, and record the actual dose delivered to the patient is the in vivo dosimetry (IVD); however, IVD is not used routinely for proton radiation therapy, despite physical and technical quality assurance protocols having been proposed and clinically investigated [46]. The present study, through dose measurements in a phantom, allowed us to assess the feasibility of applying a well-established dosimetric method with a conventional photon beam for IVD in a non-standard radiation beam. In order to improve the experimental reliability, the critical positioning uncertainties of the TLDs, which might impact on the accuracy of the dose measures and the interpretation of the trials, could be improved through the combined use of dosimetric instruments (TLDs, ionization chambers, film dosimetry, etc.).

The obtained results encourage further testing of our dosimetric system in in vivo studies. All of the experiments in the present study showed that physical dosimetry performed with TLD is reliable if the dosimeter position is carefully set and monitored. Within the framework of the MoVe IT project, the next objective is to characterize the dosimeters by performing a calibration curve across a wider dose range up to 30 Gy, as required for more complex in vivo experiments.

4. Conclusions

The current study assesses the feasibility of using thermoluminescent dosimeters (TLDs-100 type) in combination with biophysical models to assess RBE values in proton therapy beams. The results of the in vitro experiments will be essential in correctly designing and implementing the next in vivo experimental phase, as planned in the MoVe IT workflow. The study allowed the dosimetric tool and method based on the TLDs-100 to be optimized, offering the opportunity to verify and store the dosimetric information with high spatial resolution.

Author Contributions: Conceptualization, V.D., F.T., and M.P.; methodology, V.D., S.L., and M.P.; software, V.D.; validation, V.D., F.T., and S.L.; formal analysis, V.D.; investigation, V.D. and M.P.; resources, M.P.; data curation, V.D. and G.L.V.; writing—original draft preparation, V.D. and M.P.; writing—review and editing, V.D., G.L.V., and M.P.; visualization, V.D., F.T., G.L.V., S.L., and M.P.; supervision, M.P.; project administration, M.P.; funding acquisition, M.P. All authors have read and agreed to the published version of the manuscript.

Funding: This work was partially supported by the INFN CSN5 "MoVe IT"–Modeling and Verification for Ion Beam Treatment Planning.

Institutional Review Board Statement: Not applicable. This study did not involve humans or animals.

Informed Consent Statement: Not applicable.

Data Availability Statement: The data presented in this study are available on request from the corresponding author. The data are not publicly available due to the non-exclusive ownership by the authors.

Acknowledgments: We thank Emanuele Scifoni for setup optimization and insightful discussions on the data interpretation.

Conflicts of Interest: The authors declare no conflict of interest.

References

1. Yuan, T.Z.; Zhan, Z.J.; Qian, C.N. New frontiers in proton therapy: Applications in cancers. *Cancer Commun.* **2019**, *39*, 61. [CrossRef]
2. Cotter, S.E.; McBride, S.M.; Yock, T.I. Proton radiotherapy for solid tumors of childhood. *Technol. Cancer Res. Treat.* **2012**, *11*, 267–278. [CrossRef] [PubMed]
3. International Commission on Radiation Units and Measurements (ICRU). ICRU Report 78, Prescribing, recording and reporting proton beam therapy. *J. Int. Commun. Radiat. Units Meas.* **2007**, *7*, 210.
4. Paganetti, H. Proton Relative Biological Effectiveness—Uncertainties and Opportunities. *Int. J. Part. Ther.* **2018**, *5*, 2–14. [CrossRef]
5. Paganetti, H.; van Luijk, P. Biological considerations when comparing proton therapy with photon therapy. *Semin. Radiat. Oncol.* **2013**, *23*, 77–78. [CrossRef] [PubMed]
6. Tommasino, F.; Durante, M. Proton radiobiology. *Cancers* **2015**, *7*, 353–381. [CrossRef]
7. Bettega, D.; Calzolari, P.; Chauvel, P.; Courdi, A.; Herault, J.; Iborra, N.; Marchesini, R.; Massariello, P.; Poli, G.L.; Tallone, L. Radiobiological studies on the 65 MeV therapeutic proton beam at Nice using human tumour cells. *Int. J. Radiat. Biol.* **2000**, *76*, 1297–1303. [CrossRef]
8. Britten, R.A.; Nazaryan, V.; Davis, L.K.; Klein, S.B.; Nichiporov, D.; Mendonca, M.S.; Wolanski, M.; Nie, X.; George, J.; Keppel, C. Variations in the RBE for cell killing along the depth-dose profile of a modulated proton therapy beam. *Radiat. Res.* **2013**, *179*, 21–28. [CrossRef]
9. Grassberger, C.; Paganetti, H. Varying relative biological effectiveness in proton therapy: Knowledge gaps versus clinical significance. *Acta Oncol.* **2017**, *56*, 761–762. [CrossRef]
10. Oden, J.; DeLuca Jr, P.M.; Orton, C.G. The use of a constant RBE=1.1 for proton radiotherapy is no longer appropriate. *Med. Phys.* **2018**, *45*, 502–505. [CrossRef]
11. Sorensen, B.S.; Overgaard, J.; Bassler, N. In vitro RBE-LET dependence for multiple particle types. *Acta Oncol.* **2011**, *50*, 757–762. [CrossRef]
12. Wedenberg, M.; Toma-Dasu, I. Disregarding RBE variation in treatment plan comparison may lead to bias in favor of proton plans. *Med. Phys.* **2014**, *41*, 091706. [CrossRef]
13. Paganetti, H.; Niemierko, A.; Ancukiewicz, M.; Gerweck, L.E.; Goitein, M.; Loeffler, J.S.; Suit, H.D. Relative biological effectiveness (RBE) values for proton beam therapy. *Int. J. Radiat. Oncol. Biol. Phys.* **2002**, *53*, 407–421. [CrossRef]
14. Antonelli, F.; Bettega, D.; Calzolari, P.; Cherubini, R.; Dalla Vecchia, M.; Durante, M.; Favaretto, S.; Grossi, G.; Marchesini, R.; Pugliese, M.; et al. Inactivation of human cells exposed to fractionated doses of low energy protons: Relationship between cell sensitivity and recovery efficiency. *J. Radiat. Res.* **2001**, *42*, 347–359. [CrossRef] [PubMed]
15. Belli, M.; Bettega, D.; Calzolari, P.; Cera, F.; Cherubini, R.; Dalla Vecchia, M.; Durante, M.; Favaretto, S.; Gialanella, G.; Grossi, G.; et al. Inactivation of human normal and tumour cells irradiated with low energy protons. *Int. J. Radiat. Biol.* **2000**, *76*, 831–839. [CrossRef] [PubMed]
16. Dalrymple, G.V.; Lindsay, I.R.; Hall, J.D.; Mitchell, J.C.; Ghidoni, J.J.; Kundel, H.L.; Morgan, I.L. The relative biological effectiveness of 138-Mev protons as compared to cobalt-60 gamma radiation. *Radiat. Res.* **1966**, *28*, 489–506. [CrossRef]
17. Manti, L.; Durante, M.; Grossi, G.; Ortenzia, O.; Pugliese, M.; Scampoli, P.; Gialanella, G. Measurements of metaphase and interphase chromosome aberrations transmitted through early cell replication rounds in human lymphocytes exposed to low-LET protons and high-LET 12C ions. *Mutat. Res.* **2006**, *596*, 151–165. [CrossRef] [PubMed]
18. Skarsgard, L.D. Radiobiology with heavy charged particles: A historical review. *Phys. Med.* **1998**, *14* (Suppl. 1), 1–19.
19. Wouters, B.G.; Lam, G.K.Y.; Oelfke, U.; Gardey, K.; Durand, R.E.; Skarsgard, L.D. RBE measurement on the 70 MeV proton beam at TRIUMF using V79 cells and the high precision cell sorter assay. *Radiat. Res.* **1996**, *146*, 159–170. [CrossRef]
20. Dalrymple, G.V.; Lindsay, I.R.; Ghidoni, J.J.; Hall, J.D.; Mitchell, J.C.; Kundel, H.L.; Morgan, I.L. Some effects of 138-Mev protons on primates. *Radiat. Res.* **1966**, *28*, 471–488. [CrossRef] [PubMed]
21. Sorensen, B.S.; Bassler, N.; Nielsen, S.; Horsman, M.R.; Grzanka, L.; Spejlborg, H.; Swakon, J.; Olko, P.; Overgaard, J. Relative biological effectiveness (RBE) and distal edge effects of proton radiation on early damage in vivo. *Acta Oncol.* **2017**, *56*, 1387–1391. [CrossRef]
22. Suckert, T.; Beyreuther, E.; Muller, J.; Azadegan, B.; Meinhardt, M.; Raschke, F.; Bodenstein, E.; von Neubeck, C.; Luhr, A.; Krause, M.; et al. Late Side Effects in Normal Mouse Brain Tissue After Proton Irradiation. *Front. Oncol.* **2020**, *10*, 598360. [CrossRef]
23. Tommasino, F. Proton beam characterization in the experimental room of the Trento Proton Therapy facility. *Nucl. Inst. Methods Phys. Res.* **2017**, *869*, 15–20. [CrossRef]
24. Tommasino, F.; Rovituso, M.; Bortoli, E.; La Tessa, C.; Petringa, G.; Lorentini, S.; Verroi, E.; Simeonov, Y.; Weber, U.; Cirrone, P.; et al. A new facility for proton radiobiology at the Trento proton therapy centre: Design and implementation. *Phys. Med.* **2019**, *58*, 99–106. [CrossRef]
25. Horowitz, Y.S. *Heavy Charged Particle Relative TL Response: Experimental Results in Thermoluminescence and Thermoluminescent Dosimetry Volume II*; CRC Press: Boca Raton, FL, USA, 1984; pp. 114–129.
26. Hoffman, W. TL Dosimetry in High LET Radiotherapeutic Fields. *Radiat. Prot. Dos.* **1996**, *66*, 243–248. [CrossRef]
27. Olko, P.; Bilski, P.; Budzanowski, M.; Molokanov, A. Dosimetry of heavy charged particles with thermoluminescence detectors—models and applicationsA. *Radiat. Prot. Dos.* **2004**, *110*, 315–318. [CrossRef] [PubMed]

28. Bilski, P. Dosimetry of densely ionising radiation with three LiF phosphors for space applications. *Radiat. Prot. Dos.* **2006**, *120*, 397–400. [CrossRef] [PubMed]

29. Berger, T.; Hajek, M.; Summerer, L.; Fugger, M.; Vana, N. The efficiency of various thermoluminescence dosemeter types to heavy ions. *Radiat. Prot. Dos.* **2006**, *120*, 365–368. [CrossRef]

30. Zullo, J.R.; Kudchadker, R.J.; Zhu, X.R.; Sahoo, N.; Gillin, M.T. LiF TLD-100 as a Dosimeter in High Energy Proton Beam Therapy—Can It Yield Accurate Results? *Med. Dos.* **2010**, *35*, 63–66. [CrossRef]

31. Kry, S.F.; Alvarez, P.; Cygler, J.E.; DeWerd, L.A.; Howell, R.M.; Meeks, S.; O'Daniel, J.; Reft, C.; Sawakuchi, G.; Yukihara, E.G.; et al. AAPM TG 191: Clinical use of luminescent dosimeters: TLDs and OSLDs. *Med. Phys.* **2020**, *47*, e19–e51. [CrossRef]

32. Liuzzi, R.; Piccolo, C.; D'Avino, V.; Clemente, S.; Oliviero, C.; Cella, L.; Pugliese, M. Dose-Response of TLD-100 in the Dose Range Useful for Hypofractionated Radiotherapy. *Dose Response* **2020**, *18*. [CrossRef]

33. Liuzzi, R.; Savino, F.; D'Avino, V.; Pugliese, M.; Cella, L. Evaluation of LiF:Mg,Ti (TLD-100) for Intraoperative Electron Radiation Therapy Quality Assurance. *PLoS ONE* **2015**, *10*, e0139287. [CrossRef]

34. Moscovitch, M. Personnel dosimetry using LiF:Mg,Cu,P. *Radiat. Prot. Dos.* **1999**, *85*, 49–56. [CrossRef]

35. Spiers, F.W. Effective atomic number and energy absorption in tissues. *Br. J. Radiol.* **1946**, *19*, 52–63. [CrossRef] [PubMed]

36. Kron, T. Thermoluminescence dosimetry and its applications in medicine—Part 1: Physics, materials and equipment. *Australas Phys. Eng. Sci. Med.* **1994**, *17*, 175–199.

37. Kron, T. Thermoluminescence dosimetry and its applications in medicine—Part 2: History and applications. *Australas Phys. Eng. Sci. Med.* **1995**, *18*, 1–25.

38. Massillon, J.L.G.; Gamboa-deBuen, I.; Brandan, M.E. Onset of supralinear response in TLD-100 exposed to ^{60}Co gamma-rays. *Phys. D Appl. Phys.* **2006**, *39*, 262–268. [CrossRef]

39. D'Avino, V.; Caruso, M.; Arrichiello, C.; Ametrano, G.; La Verde, G.; Muto, P.; Scifoni, E.; Tommasino, F.; Pugliese, M. Thermoluminescent dosimeters (TLDs-100) calibration for dose verification in photon and proton radiation therapy. In Proceedings of the SIRR 2020, Online, 25 February 2021; p. 142. [CrossRef]

40. Boscolo, D.; Scifoni, E.; Carlino, A.; La Tessa, C.; Berger, T.; Durante, M.; Rosso, V.; Kramer, M. TLD efficiency calculations for heavy ions: An analytical approach. *Eur. Phys. J. D* **2015**, *69*, 286. [CrossRef]

41. Horowitz, Y.; Olko, P. The effects of ionisation density on the thermoluminescence response (efficiency) of LiF:Mg,Ti and LiF:Mg,Cu,P. *Radiat. Prot. Dos.* **2004**, *109*, 331–348. [CrossRef]

42. Massillon-JL, G.; Gamboa-deBuen, I.; Brandan, M.E. Observation of enhanced efficiency in the excitation of ion-induced LiF:Mg,Ti thermoluminescent peaks. *J. Appl. Phys.* **2006**, *100*, 103521. [CrossRef]

43. Spurny, F. Response of thermoluminescent detectors to charged particles and to neutrons. *Radiat. Meas.* **2004**, *38*, 407–412. [CrossRef] [PubMed]

44. Devicienti, S.; Strigari, L.; D'Andrea, M.; Benassi, M.; Dimiccoli, V.; Portaluri, M. Patient positioning in the proton radiotherapy era. *J. Exp. Clin. Cancer Res.* **2010**, *29*, 47. [CrossRef] [PubMed]

45. Liebl, J.; Paganetti, H.; Zhu, M.; Winey, B.A. The influence of patient positioning uncertainties in proton radiotherapy on proton range and dose distributions. *Med. Phys.* **2014**, *41*, 091711. [CrossRef] [PubMed]

46. Parodi, K. Dose verification of proton and carbon ion beam treatments. In *Clinical 3D Dosimetry in Modern Radiation Therapy*; Mijnheer, B., Ed.; CRC Press: Boca Raton, FL, USA, 2017; pp. 589–613.